Identifying stream-aquifer exchange by temperature gradient in a Guarani Aquifer system outcrop zone

Identificação da interação rio-aquífero, por meio de gradientes de temperatura, em área de afloramento do Aquífero Guarani

Edson Cezar Wendland[1] , Alan Reis[1] , Jamil Alexandre Ayach Anache[2] , David Maycon Schimdt Rosa[1],

Gabriel de Miranda Alcântara[1], Christopher Scott Lowry[3] & Yu-Feng Forrest Lin[4]

[1]Universidade de São Paulo, São Carlos, SP, Brasil
[2]Universidade Federal do Mato Grosso do Sul, Campo Grande, MS, Brasil
[3]University at Buffalo, Buffalo, NY, USA

[4]University of Illinois at Urbana-Champaign, Urbana, IL, USA

E-mails: ew@sc.usp.br (ECW), alanreis.ar@gmail.com (AR), anache.jamil@gmail.com (JAAA), david_maycom@hotmail.com (DMSR), gabrielmalcantara@gmail.com (GMA), cslowry@buffalo.edu (CSL), yflin@illinois.edu (YFFL)

ABSTRACT

The use of temperature as a natural tracer in hydrology is noticed since the 1960s. In recent years, there has been a revival of the use of this physical property in the investigation of water cycle. The main reasons are the cost reduction of temperature measurements and the development of distributed temperature sensing. Here, we present a study of the groundwater-surface water interaction in the Onça Creek Watershed (Guarani Aquifer System outcrop) using stream discharge data and temperature as a natural tracer. Two Parshall flumes were installed 1.2 km apart to quantify stream discharge and determine groundwater contribution. We used an optic fiber cable to identify interaction locations and a probe with thermistors to measure the vertical temperature gradient and estimate flux rates. The results show a discharge difference of ~250 m³.h⁻¹ between both flumes, which we interpret as baseflow contribution. The distributed temperature sensing allowed the identification of regions with gaining behavior. Discharge rates between 200 and 300 mm.day⁻¹ were determined from vertical temperature measurements, which agrees with the streamflow data. The study demonstrated that temperature is attractive as natural tracer in tropical conditions, where the groundwater temperature is higher than the surface water temperature, especially during the winter.

Keywords: Distributed temperature sensing; Fiber optics; Streambed temperature; Guarani Aquifer system; Groundwater-surface water interactions.

RESUMO

O uso da temperatura como traçador natural em hidrologia é observado desde a década de 1960. Nos últimos anos, foi possível observar um resgate do uso desta propriedade física na investigação do ciclo da água. As principais razões são a redução de custos na medição de temperatura e o desenvolvimento da medição de temperatura distribuída. A partir deste contexto, este trabalho apresenta um estudo da interação rio-aquífero, na Bacia do Ribeirão da Onça (afloramento do Sistema Aquífero Guarani), a partir do uso de dados de vazão do curso principal e utilizando a temperatura como traçador natural. Duas calhas Parshall foram instaladas a uma distância de 1,2 km entre si, de forma a quantificar a vazão do curso principal e determinar a contribuição de água subterrânea. Um cabo de fibra ótica foi empregado para identificar regiões de contribuição da água subterrânea ao curso superficial, assim como uma sonda de temperatura, com termistores, foi utilizada para medir o gradiente de temperatura vertical e estimar as taxas de troca entre estes meios. Os resultados indicam uma diferença de vazão de ~250 m³.h⁻¹ entre as calhas, o que pode ser interpretado como contribuição do fluxo de base ao rio. O sistema de medição distribuído de temperatura (DTS) permitiu a identificação de regiões de contribuição de água subterrânea, em virtude da diferença de temperatura entre água subterrânea e superficial. Taxas de descarga de 200 a 300 mm.dia⁻¹ foram obtidas

a partir das medições pontuais de temperatura, que concordam com os valores obtidos a partir da medição de vazão. O trabalho demonstra que a temperatura pode ser utilizada como um traçador natural, mesmo em áreas tropicais, em que a temperatura da água subterrânea é superior à da água superficial, especialmente nos períodos de inverno.

Palavras-chave: Medição distribuída de temperatura; Fibra ótica; Temperatura no leito do rio; sistema Aquífero Guarani; interação rio-aquífero.

INTRODUCTION

The sustainability of the world's largest transboundary aquifers are multinational efforts, that rely on analyses of highly variable spatial and temporal processes. The Guarani Aquifer System (GAS), which underlies Argentina, Brazil, Paraguay and Uruguay, is a classic example of a transboundary aquifer systems (Gastmans et al., 2010; Richts et al., 2011). In the GAS, groundwater recharge is constrained to small outcrop zone primarily in Brazil (Araújo et al., 1999; Foster et al., 2009; Gastmans et al., 2017), while water use is disturbed among all four countries and is regulated by international treaty (Sugg et al., 2015; Tinker & Kirchheim, 2016; Sindico et al., 2018). Globally, the sustainability of these large aquifer systems are based primarily on the quantification of the volume of groundwater storage (Richey et al., 2015, Thomas et al., 2017). Where groundwater storage is controlled by the fluxes of water entering and exiting the aquifer through recharge and discharge zones. Quantifying these fluxes can be problematic, and an issue of scale, as groundwater recharge and discharge are spatially and temporally variable (Wendland et al., 2015; Blöschl et al., 2019). As a result, current research initiatives specifically focus on quantifying fluxes entering and exiting the GAS owing to the aquifers importance to the water supply in South America (Hirata et al., 2020; Hirata & Foster, 2020). Recent studies identify groundwater recharge and surface water exchange are the most important processes for managing sustainable use (Lucas et al., 2015; Lucas & Wendland, 2015; Elliot & Bonotto, 2017; Hu et al., 2017; Melo & Wendland, 2017; Batista et al., 2018). These results point to the importance of quantifying fine scale variability in groundwater recharge and discharge.

Quantifying recharge, storage and discharge of the GAS is essential to effectively manage groundwater resources as the number of transboundary municipal, industrial, and agricultural users grows (Rodríguez et al., 2013; Gonçalves et al., 2020). The complexity of the subsurface geology and uncertainties in meteorological data integrated over large spatial scales make these components difficult to calculate (Scanlon et al., 2006; Sharda et al., 2006). Thus, some studies focused on one particular mechanism: groundwater exchange through surface water connectivity (Batista et al., 2018; Elliot & Bonotto, 2017; Hu et al., 2017; Lucas et al., 2015; Lucas & Wendland, 2015; Melo & Wendland, 2017). In an increasingly agricultural landscape in the GAS outcrop zone, groundwater-surface water (GW-SW) interactions will play a critical role in transforming and retaining the nutrients introduced by agriculture (Morrice et al., 1997; Le et al., 2018; Liu et al., 2020). Previous methods to calculate SW-GW fluxes were utilized on various scales (Elliot & Bonotto, 2017; Melo & Wendland, 2017; Batista et al., 2018; Gómez et al., 2018). Ground-based monitoring and modeling and isotopic techniques were localized while remote sensing occurred

on a large scale (Santarosa et al., 2021; Gómez et al., 2018; Melo & Wendland, 2017). Remote sensing results were found to be more inaccurate than ground-based methods for local recharge rates (Lucas et al., 2015). Localized isotopes techniques are more accurate to predict recharge rates and estimate fluxes, but high costs may limit the upscaling process (Hu et al., 2017). Better methods are needed to analyze GW-SW interactions accurately at local and regional scales in the GAS.

The identification of discharge and recharge areas using heat as a tracer is an alternative way to verify the spatial-temporal variability of such processes on streams (Stallman, 1960; Bredehoeft & Papaopulos, 1965; Constantz et al., 2003; Anderson, 2005; Constantz, 2008). Distributed and discrete approaches have been used to perform such monitoring (Selker et al., 2006a; Selker et al., 2006b; Tyler et al., 2009; Saar, 2011; Schenato, 2017). The streambed temperature monitoring using a fiber optics coupled to a distributed temperature sensing device (FO-DTS) is used to identify GW-SW interaction regions. This method relies on differences in water temperature between surface and subsurface. These technique that have been applied in different regions worldwide (Lowry et al., 2007; Matheswaran et al., 2013; Vandenbohede et al., 2014; Yao et al., 2015; Huang et al., 2016). Additionally, it is possible to quantify the groundwater discharge in the stream by measuring the streambed temperature in multiple depths (Hatch et al., 2006; Schmidt et al., 2006; Schmidt et al., 2007; Swanson & Cardenas, 2011; McCallum et al., 2012; Luce et al., 2013). Thus, an efficient strategy to locate and quantify streambed flux from surficial aquifers is to couple temperatures measurements horizontally, along the river channel, with vertical profiles, at the streambed depth (Mamer & Lowry, 2013; Kurylyk et al., 2017).

The use of heat as a tracer to identify and quantify groundwater discharge in a stream of a tropical watershed inside the GAS outcrop zone is not reported in the literature and can be an alternative way for a better determination of the GW-SW mechanisms in such important aquifer system. Hence, the aims of this study are: (i) to verify the aquifer contribution in the stream by measuring the flow upstream and downstream; (ii) to identify potential points of aquifer contribution in the stream flow using FO-DTS; and (iii) to estimate the flow contribution from the aquifer using streambed temperature gradient. The results presented here are the first assessment of GW-SW interactions using temperature as a tracer in the outcrop zone of the Guarani Aquifer System.

STUDY AREA: ONÇA CREEK WATERSHED

The Onça Creek Watershed (OCW) is located between 22°10' and 22°15' S and 47°55' and 48°00' W, at the rural area of Brotas municipality, in São Paulo State (Figure 1). The 65 km² watershed consists of a creek that flows mainly over a huge sandstone packet

(Botucatu Formation) and at the watershed outlet over a basalt complex (Figure 2A). Both units were formed during the Mesozoic age (Gilboa et al., 1976; Araújo et al., 1995; Caetano-Chang, 1997;

Figure 1. Location of Onça Creek Watershed area and its regional context.

Araújo et al., 1999; França et al., 2003; Caetano-Chang & Wu, 2006; Wendland et al., 2007; Gastmans et al., 2010). The watershed is mainly occupied by agricultural land uses (eucalyptus, sugarcane, citrus, and pasture) and is located inside the Cerrado biome (Figure 2B). According to Köpper-Geiger classification, the OCW is located in a humid subtropical climate (Cwa), with a mean air temperature of 21.6 °C (Cabrera et al., 2016). The rainfall averages around 1500 mm yr^{-1}, the aquifer recharge is approximately 440 mm yr^{-1} and base flow is around 0.5 m^3 s^{-1} at the basin outflow (Lucas et al., 2015; Lucas & Wendland, 2015).
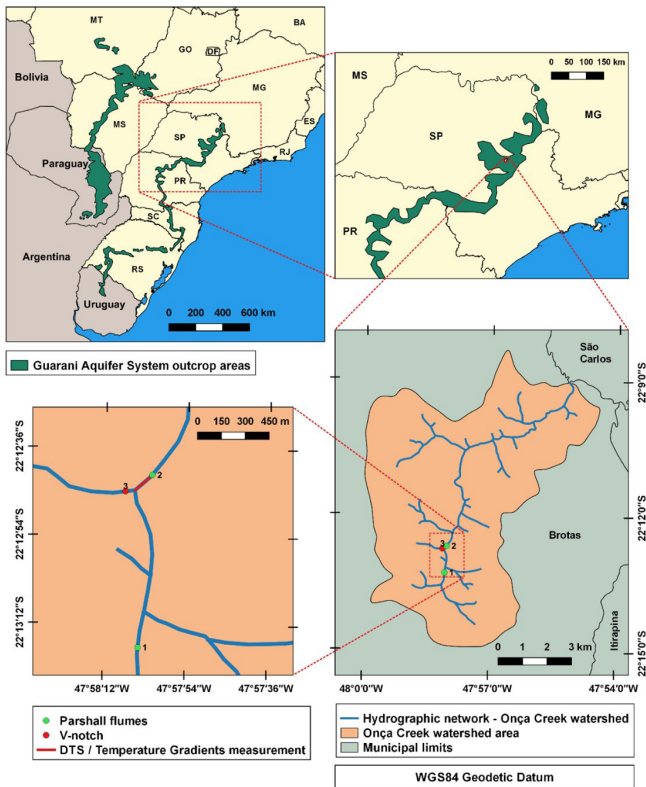
The motivation in studying GW-SW interaction in this watershed is related to its location, since all of its area is inside an outcrop zone of the Guarani Aquifer System (GAS). Considering the extent of this formation and its importance at national and international levels, the use of temperature becomes interesting for advancing the knowledge regarding the behavior of this aquifer, especially with respect to its interactions with surface flows.
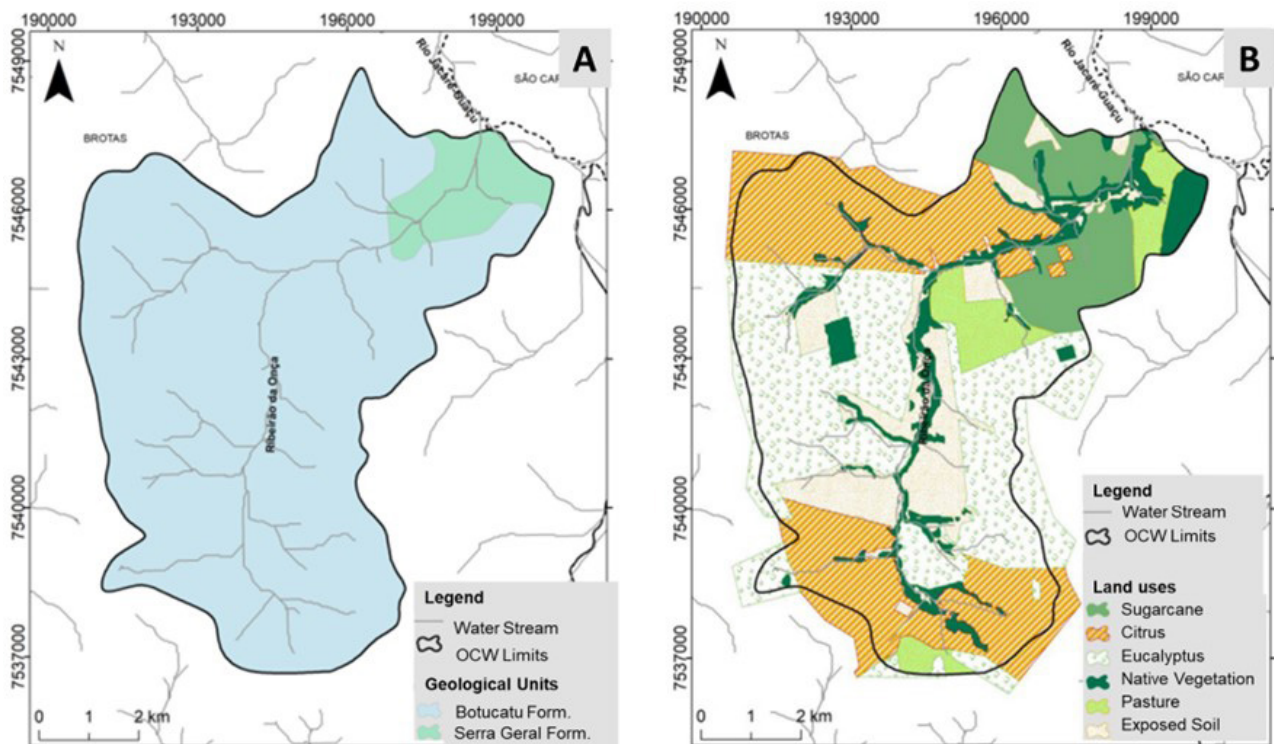
MATERIALS AND METHODS

Stream flow measurement

To quantify surface water flow, two Parshall flumes were installed in the main stream, 1.2 km apart from each other (Figure 1). One v-notch was also installed on the major affluent of Onça Creek. These three devices monitored with pressure transducers that recorded water levels every 10 minutes, allowing time series data of stream flow determination.

During the monitoring period considered here, no rainfall was detected in the study area. As a result differential stream

Figure 2. Onça Creek Watershed area: (a) geological and (b) land use and land cover maps [Source: Adapted from Coutinho (2019)].

gauging can be performed between the flumes in order to quantify groundwater baseflow contributions. Considering a simple mass balance between the Parshall flumes, baseflow in this stream reach can be calculated by (Equation 1):

$$Q_B = Q_3 - (Q_1 + Q_2) \tag{1}$$

Where:

Q_B: base flow rate (m³.h⁻¹);
Q_3: flow rate measured in the downstream Parshall flume (m³.h⁻¹);
Q_1: flow rate measured in the upstream Parshall flume (m³.h⁻¹);
Q_2: flow rate measured in the v-notch installed in the main affluent (m³.h⁻¹).

Base flow rate data can be used to estimate an average groundwater discharge rate in the river, considering a ratio between the flow rate and the streambed average area (Equation 2). This area is the product between the wetted perimeter and the stream length considered.

$$q = \frac{Q_B}{A} = \frac{Q_B}{P \times L} \tag{2}$$

Where:

q: groundwater discharge rate (m.day⁻¹);
Q_B: base flow rate (m³.h⁻¹);
A: streambed average area (m²), resulted from the product of the wetted perimeter (, in meters) and the stream length (L, in meters) considered.

In terms of water volume, an average linear rate can be calculated by relating the base flow volume drained during a day and the stream length considered (Equation 3).

$$q_{vol} = \frac{Q_B}{L} \tag{3}$$

Where:

q_{vol}: average volume of groundwater discharged per meter of stream, per day (m³.m⁻¹.day⁻¹);
Q_B: base flow rate (m³.h⁻¹);
L: stream net length, considering main channel and all affluents (m).

Distributed temperature sensing (FO-DTS) using fiber optics

Distributed Temperature Sensing (DTS) is a recent technology that allows temperature monitoring in a finer spatial (< 1 meter) and temporal resolution (< 5 seconds), when compared with punctual measurements. Using fiber optics as a sensor, placed along the streambed where it is desired to know temperature variations, the DTS device is connected and a laser pulse is sent down cable. Part of this signal returns to its origin, as a result of scattering phenomenon. This scattered signal is divided in two wavelengths, one with higher frequency (known as anti-Stokes) and other with lower frequency (known as Stokes). While the anti-Stokes is influenced by external temperature, the second is not affected by this physical property. The rate between these two plots allows temperature determination in a cable section (Selker et al., 2006a; Selker et al., 2006b; Lowry et al., 2007; Tyler et al., 2009).

A fiber optic (FO) connected to a DTS (Sensornet Oryx SR DTS system) was installed in the streambed of the main stream in the Onça Creek watershed during June 2017. Streambed temperature was measured by laying approximately 180 m of fiber-optic cable just above the sediment-water interface, upstream from the second Parshall flume. To avoid deplanements and to maintain the installation position, the fiber optic cable was tied with nylon wires and staked down to the streambed. This stakes were placed approximately every meter along the streambed.

The experimental design used at Onça Creek was a duplexed single-ended configuration (Hausner et al., 2011). From the DTS device, the cable pass through two references sections (hot bath and cold bath), with different known temperatures, these reference sections provide a calibration point above and below the target temperatures in the stream. After the reference baths, the cable enters the river and travels approximately 180 m. At the end of the cable there is a turnaround in the fiber, the path takes the reverse direction and ends passing through the two baths, without a second connection with the DTS instrument. Once installed, the location of the cable on the streambed was georeferenced using a GPS.

The FO-DTS ran during approximately 72 hours, from July, 5th, 2017 – 12:06 to July, 7th, 2017 – 09:36. Considering the device employed (Figure 3), with a sampling resolution of 0.5 m and a spatial resolution of 1.0 m, a ± 0.03°C temperature precision was obtained for every fiber optic cable meter (Sensornet, 2022).

Shallow streambed temperature gradient

To complement these data obtained from DTS and to estimate groundwater upwelling and downwelling rates from streambed temperature gradient, point temperature measurements were performed in the same stretch were the fiber optic was employed. This data collection was performed in July, 5th, 2017, simultaneously of FO-DTS employment, at 49 points, georeferenced with a GPS. The instruments used in this phase were a thermometer with a data logger embedded, connected with four thermocouples, attached to a nonconductive rod and spaced by 10 cm from each other (Figure 4). For temperature readings,

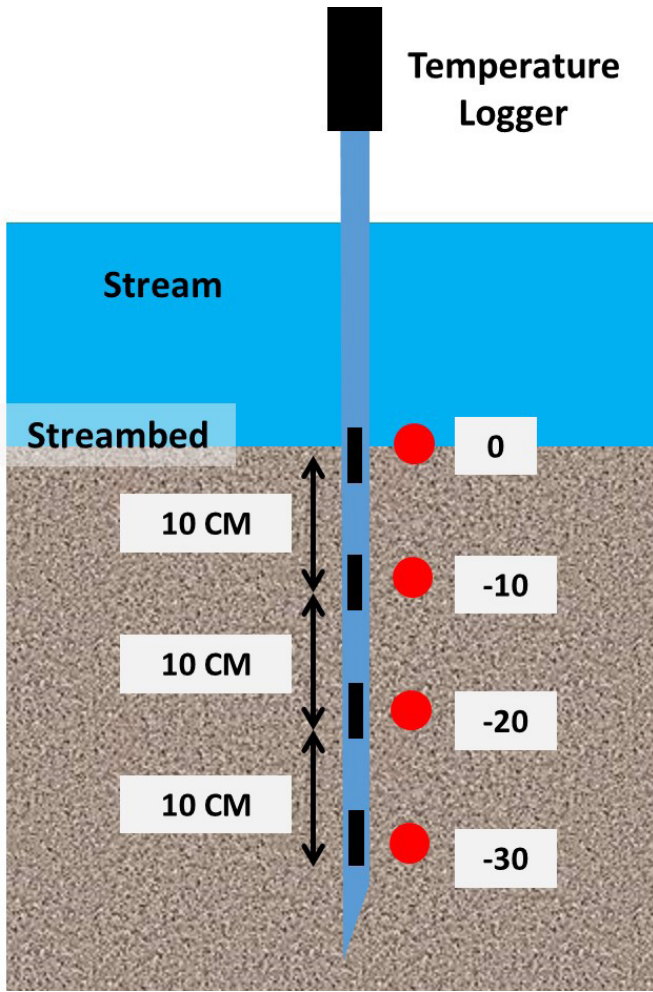**Figure 3.** DTS device employed in the Onça Creek Watershed.

Figure 4. Scheme of punctual streambed temperature measurement.

the stick was placed in way that uppermost thermocouple would be aligned with the streambed interface, while the lower three would be below the sediment water boundary. Four temperature values (one for each thermocouple) were recorded in each point, which permits the gradient temperature determination and a complementary identification and confirmation of stream-aquifer interaction points.

To estimate groundwater upwelling and downwelling rates, we use the analytical solution (Equation 4) for the transient heat and fluid flow through isotropic, homogenous, and fully saturated porous medium, proposed originally by Bredehoeft & Papaopulos (1965). This solution was implemented in a Microsoft Office Excel spreadsheet and the β value was optimized, for the function in Equation 5, using the Solver tool, based on Arriaga & Leap (2006) and Kurylyk et al. (2017). With the optimized β value, groundwater upwelling and downwelling rates were calculated using Equation 6.

$$\frac{T_z - T_0}{T_L - T_0} = f\left(\beta, \frac{z}{L}\right) = \frac{e^{\beta(z/L)} - 1}{e^{\beta} - 1} \tag{4}$$

$$F(\beta) = \sum_{z=0}^{z=L} \left[\frac{T_z - T_o}{T_L - T_o} - \frac{e^{\beta(z/L)} - 1}{e^{\beta} - 1} \right]^2 \tag{5}$$

$$q_z = \frac{k\beta}{c_w \rho_w L} \tag{6}$$

Where:

T_z: streambed temperature (°C), at a depth z, located between $z = 0$ and $z = $ L;

$\beta = \frac{c_w \rho_w q_z L}{k_e}$: corresponds to Peclet number, dimensionless parameter, which relates heat advection and diffusion. It can assume positive and negative values, according to the direction of groundwater (positive for recharge / negative for discharge);

L: characteristic dimension (cm), which is the distance between the two extremes temperature measurement points ($z = 0$ and $z = $ L). In our case, L corresponds to 30 cm;

q_z: groundwater upwelling/downwelling rates (mm.day^{-1});

k: thermal conductivity of soil (J.s^{-1}.cm^{-1}.°C^{-1}). We considered, in our case k = 1,68. 10^{-2} J.s^{-1}.cm^{-1}.°C^{-1}, that is the typical value for sand and gravel outwash aquifers (Arriaga & Leap, 2006);

c_w: specific heat of groundwater (J.kg^{-1}.°C^{-1}), considered equal to 4190 J.kg^{-1}.°C^{-1};

ρ_w: specific mass of groundwater (kg.m^{-3}), considered equal to 1000 kg.m^{-3}.

The results of β optimization can be shown in a graph, relating the values of $\frac{z}{L}$ and the function $f\left(\beta, \frac{z}{L}\right)$ similar to the example shown in Figure 5. A curve concave up indicates positive values for β and q_z, corresponding to downwelling, from the surface to the aquifer. A downward concave curve indicates the inverse, with negative values for β and q_z, and, respectively, upwelling of groundwater in the creek.

Considering the data obtained from FO-DTS measurements, we plotted a spatiotemporal graph that presents the streambed temperature variation during the deployment period. From this graph, it was possible to identify anomalies in this physical property that indicates GW-SW interactions. As the measurements were made during the winter, we observed that groundwater have higher temperatures than surface water. Then, when the interaction between these two different origin waters occurs, traces of higher temperatures are detected by FO-DTS devices installed in the streambed.

The groundwater discharge points detected by FO-DTS measurements can be confirmed with the vertical temperature gradient measurements. Higher gradients usually indicates an effluent condition, where groundwater discharges into the river. Lower gradients generally indicates an influent condition, where surface water temperature is preserved along the depth, indicating an contribution to subsurface flow (Sophocleous, 2002). Nevertheless, it is important to confirm these condition with a groundwater flux estimation, using the methodology previously explained.

RESULTS AND DISCUSSION

Stream flow measurements

The flow rates measured in the two Parshall flumes and the v-notch installed in Onça Creek watershed show gaining conditions in the stream (Figure 6). The period showed (from July, 5th to July, 8th) includes only the days when the FO-DTS
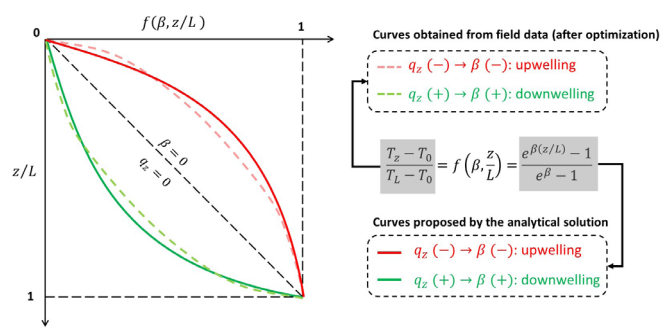
Figure 5. Examples of typical curves matching of the function $f(\beta, z/L)$.
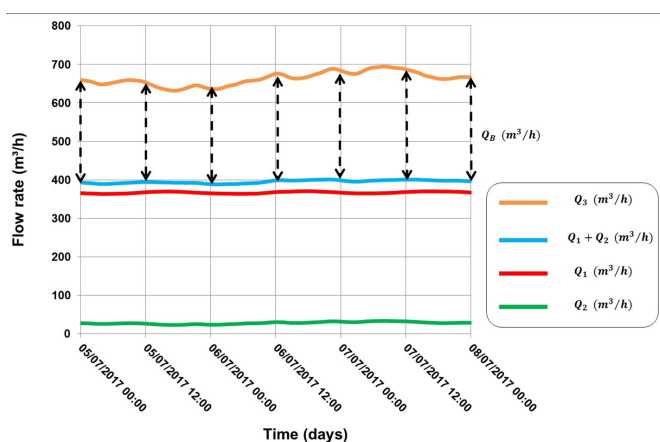

Figure 6. Flow rates measured in the Onça Creek Watershed devices, during FO-DTS employment.

measurements were performed. The red (Q_1) and the orange (Q_3) lines indicates the values obtained in the upstream and downstream Parshall flumes, respectively. The green line (Q_2) indicates flow rates visualized in the main affluent. An additional line (blue line, $Q_{1+}Q_2$) indicates the upstream flow rate, as the sum of upstream and the affluent values. The difference (Equation 1) between this sum and the downstream flow rates are the base flow rates (Q_B), highlighted by the black arrows. An average increase in stream flow of 250 $m^3.h^{-1}$ was calculated in the river stretch. This increase is directly linked to the interaction between stream and aquifer and indicates the significant diffuse contribution of groundwater in the creek. Riparian evapotranspiration influences the flow rate at the downstream section, causing the variations observed in the orange line.

Considering the Equations 2-3, intended for estimate groundwater discharge rates from base flow data, we considered 5.55 km (or 5550 m) as the creek length (main channel and all tributary length included) and a wetted perimeter of 4.5 m, with 2.5 m being from channel bottom and 1 m from each channel sides. In this way, we obtained an average groundwater discharge rate of 240 $mm.day^{-1}$. In terms volume, we obtained an average linear rate of 1.1 $m^3.(day.m)^{-1}$, which means that approximately 1.1 m^3 of groundwater is discharged in Onça Creek along each meter of its length per day. These results are close to the values

calculated with the temperature gradients, as will be seen in the section "Results – Shallow streambed temperature gradient".

Spatial and temporal fluctuations in temperature using FO-DTS

The profile obtained from FO-DTS deployment are shown in the Figure 6. This graph is divided in two parts, considering the path traveled by the fiber optic cable. The x-axis distance takes into account all the cable length used, since the reference sections (~20 m each) for calibration and its return to the initial point (~140 m in each way). The temperature scale was reduced to the interval between 16 to 20°C, to highlight possible temperature anomalies, that indicates possible stream-aquifer interactions. These data show the daily temperature variation in the streambed, with hot (predominantly red zones) and cold (predominantly blue zones) graph regions, interspersed in the horizontal direction.

The vertical columns, in specific regions, represent the temperature anomalies. These anomalies are hotter zones, indicating the groundwater discharging into the stream. This condition is persistent during the measurement time, considering the groundwater thermal stability. They are presented in Figure 7 in a mirrored form, looking its two parts, considering the path traveled by the fiber optic cable.

Streambed temperature data shows a pattern of 10 vertical columns (Figure 6), indicating temperature anomalies and possible points of stream-aquifer interaction. Most of them (five anomalous columns) are located between x = 60 and x = 90 m (or between x = 260 and x = 290, in the return signal), which can be indicated as a potential zone of groundwater discharge, considering the proximity between these columns. A second region of high groundwater discharge (three anomalous columns) can be identified in last meters of the cable, after x = 165 m (or near x = 190 m, in the return signal). Isolated discharge points are also visible, near x = 45 m (or x ~ 320 m), near x = 110 m (or x ~ 250 m) and near x = 130 m (or x ~ 225 m).

Shallow streambed temperature gradient

The vertical temperature gradients measurements obtained in Onça Creek streambed resulted in Figure 8. The gray bars indicate the gradients, while the colored circles indicates the temperatures in each depth (0 cm, -10 cm, -20 cm, -30 cm) used for the gradient determination. If the colored circles are separated from each other, we can see higher values in the gray bar, indicating an increased temperature variation. On the other hand, when the colored circles are close to each other, the bars present low values, indicating small or no variation in vertical temperature. The stream linear distance, presented in the x-axis, represents the same locations where the fiber optics cable was installed. It is important to remember that these measurements was made point to point, with the procedures commented in the methodology section.

The vertical temperature gradients varies between 0.67 and 14.33 $°C.m^{-1}$. The shallow temperatures (0 cm – dark blue circles) represent an approximately constant temperature of the surface
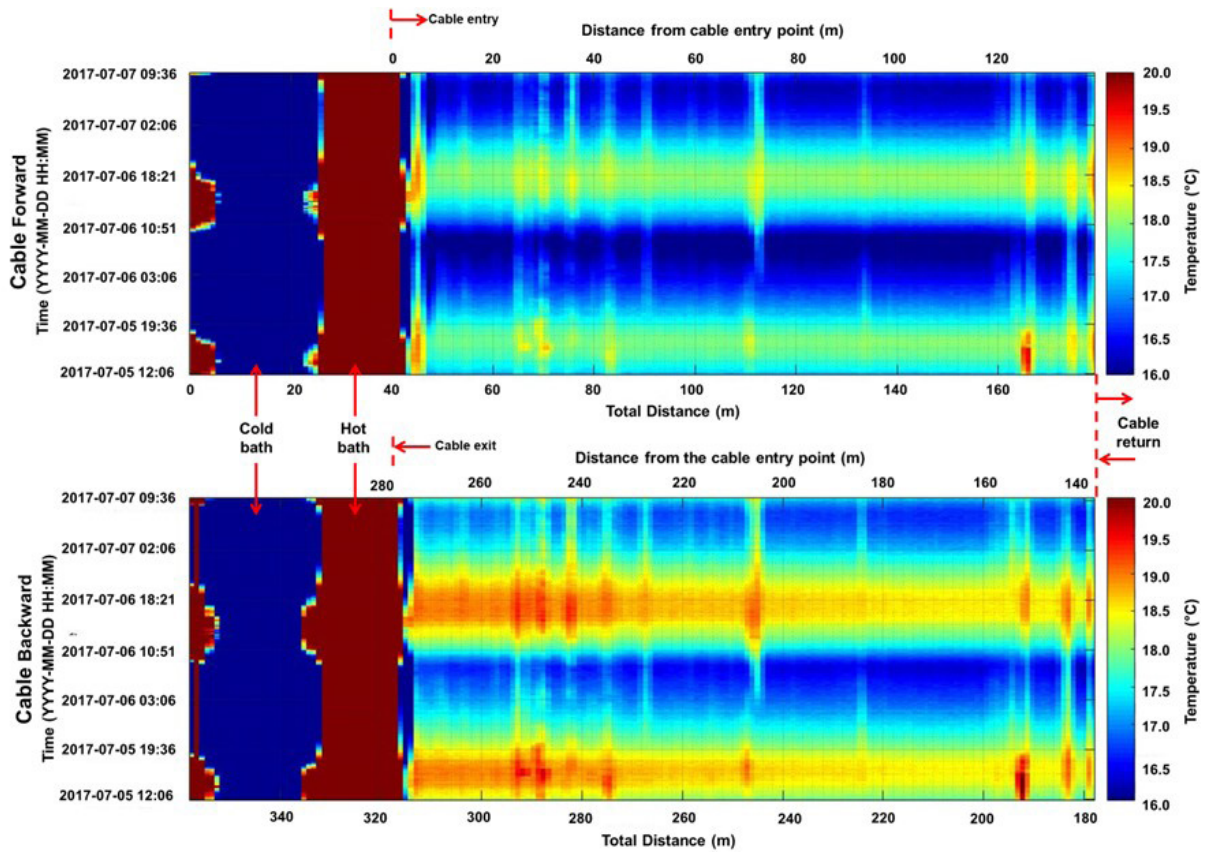
Figure 7. Spatiotemporal FO-DTS temperature traces at Onça Creek (from July, 5th, 2017 – 12:06 to July, 7th, 2017 – 09:36).
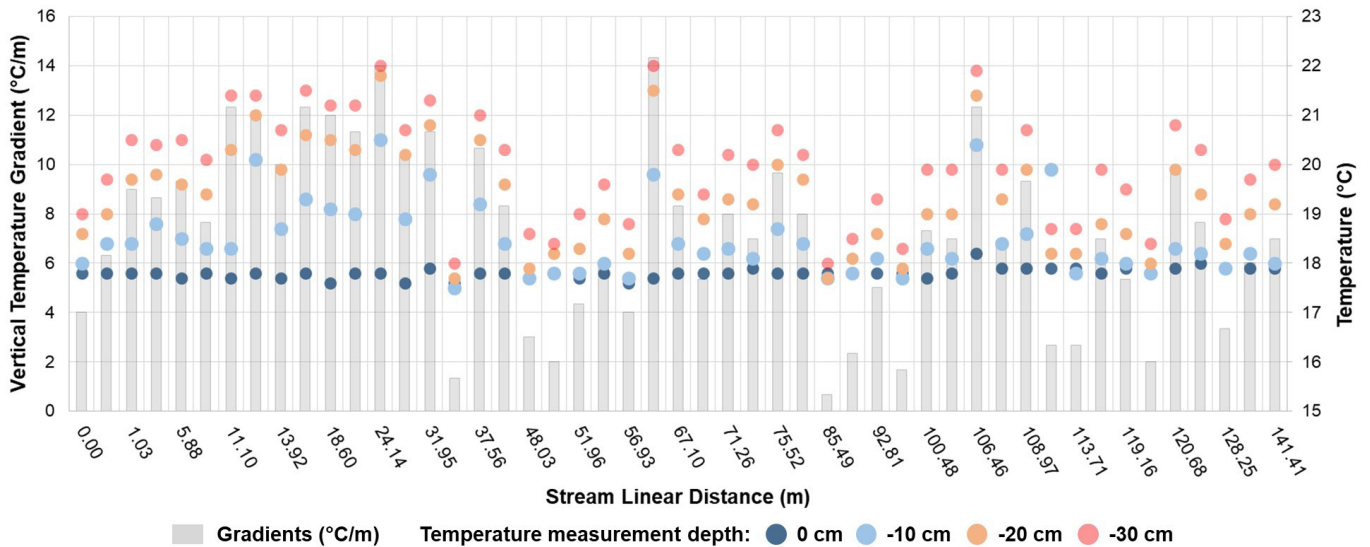

Figure 8. Temperatures and gradients obtained from punctual measurements in Onça Creek streambed.

water. Considering the other depths, the variations are stronger, with no visible trend. Most of the measurement points show an increase in the temperatures with the depth, respecting a general trend, considering both the presence of Earth's geothermal gradient and a higher and stable groundwater temperature. In some points (ex.: x = 37.42 m and x = 85.49 m), the temperatures in intermediate depths are lower or even very close to the value obtained at 0 cm depth. On the other hand, the deepest temperature (30 cm) was

slightly higher when compared with the other three, creating a low temperature gradient. This situation can indicate groundwater recharge conditions.

To confirm the GW-SW interaction condition, we obtained the groundwater flux considering the analytical solution for heat and fluid flow in porous medium (Bredehoeft & Papaopulos, 1965). The results are shown in the Figure 9a-9b. In Figure 9a, the gray bars indicate the vertical temperature gradient, while the
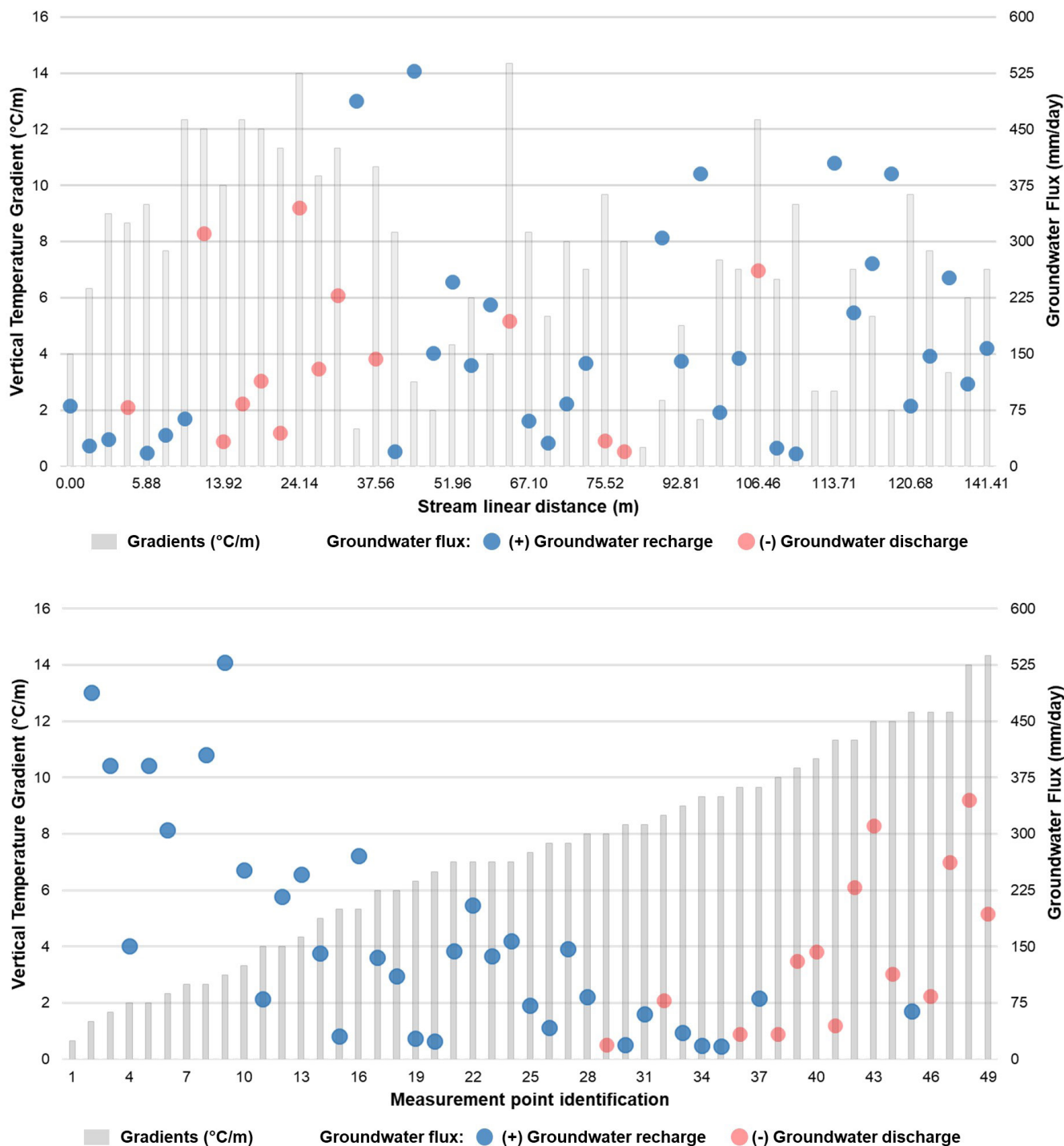
Figure 9. Gradients and groundwater flux values obtained from punctual measurements in Onça Creek streambed: (a) ordered by position (b) in ascending order of gradients.

colored circles indicate the groundwater flux values. Red circles indicate an effluent condition (groundwater discharges in the stream) and dark blue circles indicate an influent condition (stream recharges aquifer).

We can see from the results two different conditions along the stream, which shows a variability in the GW-SW interaction behavior. Two regions of effluent condition are highlighted: between the points

x = 12.17 m and x = 31.59 m and also between x = 75.52 m and x = 84.67 m. Both regions present high vertical temperature gradient, up to 8°C.m⁻¹. Other isolated points with discharge condition are found at x = 62.81 m and at x = 106.46 m, where high vertical temperature gradient values are also found. Other regions

and isolated points presents the influent condition, which different gradient values, which did not exceed 15 °C.m⁻¹. Figure 9b

shows the same results of the previous graph, but with vertical temperature gradient ordered from lowest to highest values. We clearly notice that the results respect the tendency that low temperature gradients indicates an influent condition (dark blue circles), while high gradients are indicative of an effluent condition (red circles).

The highest value for groundwater recharge flux is 525 mm.day^{-1}, which does not necessary occur in the lowest vertical temperature gradient. As these rates were determined from an optimization, the results do not always respect the direct relationship between gradient and the rates occurred in the river-aquifer interaction. However, in general, considering all evaluated points, we can notice a decrease tendency of this flux with the gradient increase. For groundwater discharge, the highest rate (345 mm.day^{-1}) was found for the second highest temperature gradient, which can also be linked to the optimization quality variation. In the same way, we perceive a general increased trend in recharge fluxes with the growing of temperature gradients.

The first point of groundwater discharge flux appears with a vertical temperature gradient of 8 °C.m^{-1} approximately. From this threshold, most of gradients are linked to groundwater discharges. However, it is still possible to observe some points of groundwater recharge beyond the 8 °C.m^{-1}. These points are contrary to the expected trend, with higher gradients indicating groundwater discharge conditions. When we observe the optimization results of these points, we noticed that $F(\beta)$ finds a result, that is not the most adequate. While the analytical solution used reproduces an exponential curve, with a unique concavity, giving sign to β, that indicates the condition in that point (discharge/recharge), the field data in these points forms a curve with alternation of concavity. In this way, points with vertical temperature gradient upper to 8 °C.m-1, that indicates groundwater recharge condition, are inconsistent.

Some reasons that explains this fact are possibly linked to the lack of uniformity in the saturated medium material at which the temperature was measured, specially thermal parameters (Cuthbert et al., 2010), which implies disregarding the assumptions considered by the analytical solution used, providing inadequate results. Other possibility is linked to groundwater contribution from creek banks (Anibas et al., 2011), affecting the temperature gradients punctually measured at the channel bottom, considering convective heat transport. Finally, inadequate positioning of the thermocouples in the streambed (Irvine et al., 2017), leading to temperatures that are not representative of the interaction zone. An occurrence of a transient temperature zone (referred as extinction depth), influenced by periodic signals, as diurnal oscillation, can also possible cause of this concavity changing at these specific points (Briggs et al., 2014; Swanson & Cardenas, 2011).

Considering the optimizations performed to determine the interaction rates, and the respective occurrences of concavity changes, we observed that a transition interval, in which the influent condition (occurrence of blue circles in Figure 9b) would no longer occur, is between 8 and 10 °C.m^{-1}. Thus, gradients above this range should indicate groundwater discharge into the stream.

Considering previous works in Onça Creek watershed (Arantes et al., 2006), groundwater discharge flux were quantified using seepage meters, in three sections, downstream to the stretch analyzed in this work. The average rates obtained by them in this sections was 175.01 mm.day^{-1} (Section 1 – downstream section); 290.15 mm.day^{-1} (Section 2) and 556.45 mm.day^{-1} (Section 3 – upstream section). Previous research show increasing rate in the downstream-upstream direction. Considering the estimates from this study with the vertical temperature gradient monitoring, both results present the same order of magnitude. The increased trend in downstream-upstream direction was not confirmed, considering that our results comprises a smaller stream length, even being in a upstream stretch from their reference sections. Changes in land cover, land use and variations in rainfall regime possibly affected by climate change can also be responsible for this reduction in influent condition rates.

Comparing stream flow with temperature measurements (FO-DTS and vertical temperatures)

As commented in section "Results – Stream flow measurements", the results from stream flow measurements and from shallow streambed temperature gradient present the same order of magnitude. Stream flow measurements indicate an average groundwater rate of 240 mm.day^{-1}, while point temperature measurements provided a value of 345 mm.day^{-1} as the maximum rate calculated, with some points with rates between 100 and 200 mm.day^{-1}. Both results are consistent with previous data from the same watershed. Some uncertainties, as possible measurements failures, in both flow rates and temperature gradients; and those linked to the optimization quality, can be the causes for these different results.

The Figures 7 and 9a together allows us the comparison between distributed and point temperature sensing. We highlight that there is a difference in the main x-axis (bottom axes) in these two figures. In Figure 9a, we do not have the calibration sections. However, if we use the secondary x-axis in Figure 7 (top axis), comparing with the main axis in Figure 9a, we are looking to the same points. We can notice that almost all temperature anomalies detected by FO-DTS (Figure 7) are coincident with points of groundwater discharge rates (Figure 9a), which proves the efficiency of FO-DTS devices to find locations with this feature. The exception was the temperature anomalies detected by FO-DTS in the last meters fiber optic cable, where the punctual measurements indicates recharge rates (from x = 125m to x = 140 m). In this case, it is possible that the gradients measured was not in the same points, or in the same sections, where the anomalies were detected by the FO-DTS.

CONCLUSION

This paper presented an experimental approach concerning the use of temperature as a natural tracer of stream-aquifer interaction in a tropical basin. Distributed Temperature Sensing using a fiber optic cable (FO-DTS) allowed us to identify points where groundwater discharge occurs, due to the temperature anomalies created by the stream-aquifer interaction, when compared with the surrounding points. Different from temperate zones, these anomalies are hotter zones, once groundwater presents higher

temperature than surface water, during the winter in Brazil, which is located in a tropical zone.

Additional methods were applied to estimate the GW-SW interaction rates. From stream flow data, we estimated an average groundwater discharge rate of 240 mm.day^{-1} and an average linear rate of 1.1 m^3.(day.m)$^{-1}$. This result are close with the rates obtained from vertical temperature gradients, considering the use of the analytical solution for the transient heat and fluid flow. Considering groundwater discharge, a maximum rate of 345 mm.day^{-1} was detected from these point measurements, while minor values was also observed, matching with the average value calculated form stream flow data. Groundwater recharge was also detected, mainly coinciding with low temperature gradients, with a maximum rate of 525 mm.day^{-1}.

In terms of vertical temperature gradients, we noted a variation from 0.67 and 14.33 °C.m^{-1}, along the river stretch analyzed. A change of condition, from groundwater recharge to groundwater discharge, was observed with gradients between 8 to 10 °C.m^{-1}. In some points where point temperature measurements were made, we noted a recharge condition with high temperature gradients. In these points, the analytical solution did not match the field data measured, which presented both concavities. Non-uniform streambed materials, disregarding the assumptions considered by the analytical solution used; groundwater contributions from the creek banks, changing temperature gradients; and thermocouple positioning failures; are possible explanations for this inconsistent results.

We noticed that temperature, both in terms of distributed and point measurements, can be used as tool to identify GW-SW interactions in tropical basins, especially in an outcrop area of Guarani Aquifer System. It is important to be aware of the limitations involved in each method, such as the additional methods need when using FO-DTS to determine interaction rates and the possibility of disregarding assumptions made by solutions implemented with temperature gradient data. The results will be useful for future works, using temperature as natural tracer in tropical zones, and for recharge evaluation in Guarani Aquifer System.

ACKNOWLEDGEMENTS

REFERENCES

Anderson, M. P. (2005). Heat as a ground water tracer. *Ground Water*, *43*(6), 951-968. http://dx.doi.org/10.1111/j.1745-6584.2005.00052.x.

Anibas, C., Buis, K., Verhoeven, R., Meire, P., & Batelaan, O. (2011). A simple thermal mapping method for seasonal spatial patterns of groundwater–surface water interaction. *Journal of Hydrology*, *397*(1-2), 93-104. http://dx.doi.org/10.1016/j.jhydrol.2010.11.036.

Arantes, E. J., Chaudhry, F. H., & Marcussi, F. N. (2006). Caracterização da interação entre rio e aquífero. *Águas Subterrâneas*, *20*(2), 97-108. https://doi.org/10.14295/ras.v20i2.11728.

Araújo, L. M., França, A. B., & Potter, P. E. (1995). *Arcabouço hidrogeológico do aquífero gigante do Mercosul (Brasil, Argentina, Uruguai e Paraguai): formações Botucatu, Pirambóia, Rosário do Sul, Buena Vista, Misiones e Tacuarembó. Águas Subterrâneas.* Retrieved in 2022, June 28, from https://aguassubterraneas.abas.org/asubterraneas/article/view/22488

Araújo, L. M., França, A. B., & Potter, P. E. (1999). Hydrogeology of the Mercosul aquifer system in the Paraná and Chaco-Paraná Basins, South America, and comparison with the Navajo Nugget aquifer system, USA. *Hydrogeology Journal*, *7*, 317-336. http://dx.doi.org/10.1007/s100400050205.

Arriaga, M. A., & Leap, D. I. (2006). Using solver to determine vertical groundwater velocities by temperature variations, Purdue University, Indiana, USA. *Hydrogeology Journal*, *14*(1), 253-263. http://dx.doi.org/10.1007/s10040-004-0381-x.

Batista, L. V., Gastmans, D., Sánchez-Murillo, R., Farinha, B. S., Santos, S. M. R., & Chang, H. K. (2018). Groundwater and surface water connectivity within the recharge area of Guarani aquifer system during El Niño 2014-2016. *Hydrological Processes*, *32*(16), 2483-2495. http://dx.doi.org/10.1002/hyp.13211.

Blöschl, G., Bierkens, M. F. P., Chambel, A., Cudennec, C., Destouni, G., Fiori, A., Kirchner, J. W., McDonnell, J. J., Savenije, H. H. G., Sivapalan, M., Stumpp, C., Toth, E., Volpi, E., Carr, G., Lupton, C., Salinas, J., Széles, B., Viglione, A., Aksoy, H., Allen, S. T., Amin, A., Andréassian, V., Arheimer, B., Aryal, S. K., Baker, V., Bardsley, E., Barendrecht, M. H., Bartosova, A., Batelaan, O., Berghuijs, W. R., Beven, K., Blume, T., Bogaard, T., Amorim, P. B., Böttcher, M. E., Boulet, G., Breinl, K., Brilly, M., Brocca, L., Buytaert, W., Castellarin, A., Castelletti, A., Chen, X., Chen, Y., Chen, Y., Chifflard, P., Claps, P., Clark, M. P., Collins, A. L., Croke, B., Dathe, A., David, P. C., Barros, F. P. J., Rooij, G., Baldassarre, G., Driscoll, J. M., Duethmann, D., Dwivedi, R., Eris, E., Farmer, W. H., Feiccabrino, J., Ferguson, G., Ferrari, E., Ferraris, S., Fersch, B., Finger, D., Foglia, L., Fowler, K., Gartsman, B., Gascoin, S., Gaume, E., Gelfan, A., Geris, J., Gharari, S., Gleeson, T., Glendell, M., Bevacqua, A. G., González-Dugo, M. P., Grimaldi, S., Gupta, A. B., Guse, B., Han, D., Hannah, D., Harpold, A., Haun, S., Heal, K., Helfricht, K., Herrnegger, M., Hipsey, M., Hlaváčiková, H., Hohmann, C., Holko, L., Hopkinson, C., Hrachowitz, M., Illangasekare, T. H., Inam, A., Innocente, C., Istanbulluoglu, E., Jarihani, B., Kalantari, Z., Kalvans, A., Khanal, S., Khatami, S., Kiesel, J., Kirkby, M., Knoben, W., Kochanek, K., Kohnová, S., Kolechkina, A., Krause, S., Kreamer, D., Kreibich, H., Kunstmann, H., Lange, H., Liberato, M. L. R., Lindquist, E., Link, T., Liu, J., Loucks, D. P., Luce, C., Mahé, G., Makarieva, O., Malard, J., Mashtayeva, S., Maskey, S., Mas-Pla, J., Mavrova-Guirguinova, M., Mazzoleni, M., Mernild, S., Misstear, B. D., Montanari, A., Müller-Thomy, H., Nabizadeh, A., Nardi, F., Neale, C., Nesterova, N., Nurtaev, B., Odongo, V. O., Panda, S., Pande, S., Pang, Z., Papacharalampous, G., Perrin, C., Pfister, L., Pimentel, R., Polo, M.

J., Post, D., Sierra, C. P., Ramos, M.-H., Renner, M., Reynolds, J. E., Ridolfi, E., Rigon, R., Riva, M., Robertson, D. E., Rosso, R., Roy, T., Sá, J. H. M., Salvadori, G., Sandells, M., Schaefli, B., Schumann, A., Scolobig, A., Seibert, J., Servat, E., Shafiei, M., Sharma, A., Sidibe, M., Sidle, R. C., Skaugen, T., Smith, H., Spiessl, S. M., Stein, L., Steinsland, I., Strasser, U., Su, B., Szolgay, J., Tarboton, D., Tauro, F., Thirel, G., Tian, F., Tong, R., Tussupova, K., Tyralis, H., Uijlenhoet, R., van Beek, R., van der Ent, R. J., van der Ploeg, M., Van Loon, A. F., van Meerveld, I., van Nooijen, R., van Oel, P. R., Vidal, J.-P., von Freyberg, J., Vorogushyn, S., Wachniew, P., Wade, A. J., Ward, P., Westerberg, I. K., White, C., Wood, E. F., Woods, R., Xu, Z., Yilmaz, K. K., & Zhang, Y. (2019). Twenty-three unsolved problems in hydrology (UPH) – a community perspective. *Hydrological Sciences Journal*, *64*(10), 1141-1158. http://dx.doi.org/10.1080/02626667.2019.1620507.

Bredehoeft, J. D., & Papaopulos, I. S. (1965). Rates of vertical groundwater movement estimated from the Earth's thermal profile. *Water Resources Research*, *1*(2), 325-328. http://dx.doi.org/10.1029/WR001i002p00325.

Briggs, M. A., Lautz, L. K., Buckley, S. F., & Lane, J. W. (2014). Practical limitations on the use of diurnal temperature signals to quantify groundwater upwelling. *Journal of Hydrology*, *519*, 1739-1751. http://dx.doi.org/10.1016/j.jhydrol.2014.09.030.

Cabrera, M. C. M., Anache, J. A. A., Youlton, C., & Wendland, E. (2016). Performance of evaporation estimation methods compared with standard 20 m2 tank. *Revista Brasileira de Engenharia Agrícola e Ambiental*, *20*, 874-879.

Caetano-Chang, M. R. (1997). *A Formação Pirambóia no centro-leste do estado de São Paulo* (Habilitation thesis). Universidade Estadual Paulista "Júlio de Mesquita Filho", Instituto de Geociências e Ciências Exatas, Rio Claro.

Caetano-Chang, M. R., & Wu, F. T. (2006). Arenitos flúvio-eólicos da porção superior da Formação Pirambóia, na porção centro-leste paulista. *Revista Brasileira de Geociências*, *36*(2), 296-304.

Constantz, J. (2008). Heat as a tracer to determine streambed water exchanges. *Water Resources Research*, *44*(4), W00D10. http://dx.doi.org/10.1029/2008WR006996.

Constantz, J., Tyler, S. W., & Kwicklis, E. (2003). Temperature-profile methods for estimating percolation rates in arid environments. *Vadose Zone Journal*, *2*(1), 12-24. http://dx.doi.org/10.2136/vzj2003.0012.

Coutinho, J. V. (2019). *Caracterização geofísica e modelagem do escoamento subterrâneo em área de afloramento do Sistema Aquífero Guarani* (Master's thesis). Universidade de São Paulo, Escola de Engenharia de São Carlos, São Carlos.

Cuthbert, M. O., Mackay, R., Durand, V., Aller, M.-F., Greswell, R. B., & Rivett, M. O. (2010). Impacts of river bed gas on the hydraulic and thermal dynamics of the hyporheic zone. *Advances in Water Resources*, *33*(11), 1347-1358. http://dx.doi.org/10.1016/j.advwatres.2010.09.014.

Elliot, T., & Bonotto, D. M. (2017). Hydrogeochemical and isotopic indicators of vulnerability and sustainability in the GAS aquifer, São Paulo State, Brazil. *Journal of Hydrology: Regional Studies*, *14*, 130-149. http://dx.doi.org/10.1016/j.ejrh.2017.10.006.

Foster, S., Hirata, R., Vidal, A., Schmidt, G., & Garduño, H. (2009). The Guarani Aquifer Initiative – towards realistic groundwater management in a transboundary context. *GW Mate Case Profile Collection*, *9*, 1-28.

França, A. B., Araújo, L. M., Maynard, J. B., & Potter, P. E. (2003). Secondary porosity formed by deep meteoric leaching: Botucatu eolanite, southern South America. *The American Association of Petroleum Geologists Bulletin*, *87*, 1073-1082.

Gastmans, D., Chang, H. K., & Hutcheon, I. (2010). Groundwater geochemical evolution in the northern portion of the Guarani Aquifer System (Brazil) and its relationship to diagenetic features. *Applied Geochemistry*, *25*, 16-33. http://dx.doi.org/10.1016/j.apgeochem.2009.09.024.

Gastmans, D., Mira, A., Kirchheim, R., Vives, L., Rodríguez, L., & Veroslavsky, G. (2017). Hypothesis of groundwater fow through geological structures in Guarani Aquifer System (GAS) using chemical and isotopic data. *Procedia Earth and Planetary Science*, *17*, 136-139. http://dx.doi.org/10.1016/j.proeps.2016.12.030.

Gilboa, Y., Mero, F., & Mariano, I. B. (1976). The Botucatu Aquifer of South America, model of an untapped continental aquifer. *Journal of Hydrology*, *29*, 165-179. http://dx.doi.org/10.1016/0022-1694(76)90012-3.

Gómez, D., Melo, D. C. D., Rodrigues, D. B. B., Xavier, A. C., Guido, R. C., & Wendland, E. (2018). Aquifer responses to rainfall through spectral and correlation analysis. *Journal of the American Water Resources Association*, *54*(6), 1341-1354. https://doi.org/10.1111/1752-1688.12696.

Gonçalves, R. D, Teramoto, E. H., & Chang, H. K. (2020). Regional groundwater modeling of the Guarani Aquifer System. *Water*, *12*(9), 2323. http://dx.doi.org/10.3390/w12092323.

Hatch, C. E., Fisher, A. T., Revenaugh, J. S., Constantz, J., & Ruehl, C. (2006). Quantifying surface water–groundwater interactions using time series analysis of streambed thermal records: method development. *Water Resources Research*, *42*(10), W10410. http://dx.doi.org/10.1029/2005WR004787.

Hausner, M. B., Suárez, F., Glander, K. E., van de Giesen, N., Selker, J. S., & Tyler, S. W. (2011). Calibrating single-ended fiber-optic Raman spectra distributed temperature sensing data. *Sensors (Basel)*, *11*(11), 10859-10879. http://dx.doi.org/10.3390/s111110859.

Hirata, R., & Foster, S. The Guarani Aquifer System - from regional reserves to local use. (2020). *Quarterly Journal of Engineering*

Geology and Hydrogeology, 54(1), 1-7. http://dx.doi.org/10.1144/qjegh2020-091.

Hirata, R., Kirchheim, R. E., & Manganelli, A. (2020). Diplomatic advances and setbacks of the Guarani Aquifer System in South America. *Environmental Science & Policy, 114*, 384-393.

Hu, K., Awange, J. L., Khandu, Forootan, E., Gonçalves, R. M., & Fleming, K. (2017). Hydrogeological characterisation of groundwater over Brazil using remotely sensed and model products. *The Science of the Total Environment, 599-600*, 372-386. http://dx.doi.org/10.1016/j.scitotenv.2017.04.188.

Huang, X., Andrews, C. B., Liu, J., Yao, Y., Liu, C., Tyler, S. W., Selker, J. S., & Zheng, C. (2016). Assimilation of temperature and hydraulic gradients for quantifying the spatial variability of streambed hydraulics. *Water Resources Research, 52*(8), 6419-6439. http://dx.doi.org/10.1002/2015WR018408.

Irvine, D. J., Briggs, M. A., Lautz, L. K., Gordon, R. P., McKenzie, J. M., & Cartwright, I. (2017). Using diurnal temperature signals to infer vertical groundwater-surface water exchange. *Ground Water, 55*(1), 10-26. http://dx.doi.org/10.1111/gwat.12459.

Kurylyk, B. L., Irvine, D. J., Carey, S. K., Briggs, M. A., Werkema, D. D., & Bonham, M. (2017). Heat as a groundwater tracer in shallow and deep heterogeneous media: analytical solution, spreadsheet tool, and field applications. *Hydrological Processes, 31*(14), 2648-2661. http://dx.doi.org/10.1002/hyp.11216.

Le, A. T. T., Kasahara, T., & Vudhivanich, V. (2018). Seasonal variation and retention of ammonium in small agricultural streams in central Thailand. *Environments, 5*(7), 78. http://dx.doi.org/10.3390/environments5070078.

Liu, X., Wang, X., Zhang, L., Fan, W., Yang, C., Li, E., & Wang, Z. (2020). Impact of land use on shallow groundwater quality characteristics associated with human health risks in a typical agricultural area in central China. *Environmental Science and Pollution Research International, 28*(2), 1712-1724. http://dx.doi.org/10.1007/s11356-020-10492-x.

Lowry, C. S., Walker, J. F., Hunt, R. J., & Anderson, M. P. (2007). Identifying spatial variability of groundwater discharge in a wetland stream using a distributed temperature sensor. *Water Resources Research, 43*(10), W10408. http://dx.doi.org/10.1029/2007WR006145.

Lucas, M., & Wendland, E. (2015). Recharge estimates for various land uses in the Guarani Aquifer System outcrop area. *Hydrological Sciences Journal, 61*(7), 1253-1262. http://dx.doi.org/10.1080/02626667.2015.1031760.

Lucas, M., Oliveira, P. T. S., Melo, D. C. D., & Wendland, E. (2015). Evaluation of remotely sensed data for estimating recharge to an outcrop zone of the Guarani Aquifer System (South America). *Hydrogeology Journal, 23*(5), 961-969. http://dx.doi.org/10.1007/s10040-015-1246-1.

Luce, C. H., Tonina, D., Gariglio, F., & Applebee, R. (2013). Solutions for the diurnally forced advection–diffusion equation to estimate bulk fluid velocity and diffusivity in streambeds from temperature time series. *Water Resources Research, 49*(1), 488-506. http://dx.doi.org/10.1029/2012WR012380.

Mamer, E. A., & Lowry, C. S. (2013). Locating and quantifying spatially distributed groundwater/surface water interactions using temperature signals with paired fiber-optic cables. *Water Resources Research, 49*(11), 7670-7680. http://dx.doi.org/10.1002/2013WR014235.

Matheswaran, K., Blemmer, M., Rosbjerg, D., & Boegh, E. (2013). Seasonal variations in groundwater upwelling zones in a Danish lowland stream analyzed using Distributed Temperature Sensing (DTS). *Hydrological Processes, 28*(3), 1422-1435. http://dx.doi.org/10.1002/hyp.9690.

McCallum, A. M., Andersen, M. S., Rau, G. C., & Acworth, R. I. (2012). A 1-D analytical method for estimating surface water–groundwater interactions and effective thermal diffusivity using temperature time series. *Water Resources Research, 48*(11), 1-8. http://dx.doi.org/10.1029/2012WR012007.

Melo, D. C. D., & Wendland, E. (2017). Shallow aquifer response to climate change scenarios in a small catchment in the Guarani Aquifer outcrop zone. *Anais da Academia Brasileira de Ciências, 89*(Suppl. 1), 391-406. http://dx.doi.org/10.1590/0001-3765201720160264.

Morrice, J. A., Vallet, H. M., Clifford, N. D., & Campana, M. E. (1997). Alluvial characteristics, groundwater-surface water exchange and hydrological retention in headwater streams. *Hydrological Processes, 11*(3), 253-267. http://dx.doi.org/10.1002/(SICI)1099-1085(19970315)11:3%3C253:AID-HYP439%3E3.0.CO;2-J.

Richey, A. S., Thomas, B. F., Lo, M.-H., Reager, J. T., Famiglietti, J. S., Voss, K., Swenson, S., & Rodell, M. (2015). Quantifying renewable groundwater stress with GRACE. *Water Resources Research, 51*(7), 5217-5238. http://dx.doi.org/10.1002/2015WR017349.

Richts, A., Struckmeier, W., & Zaepke, M. (2011). WHYMAP and the groundwater resources of the world 1:25,000,000. In J. A. A. Jones (Ed.), *Sustaining groundwater resources: a critical element in the global water crisis* (pp. 159-173). Dordrecht: Springer. https://doi.org/10.1007/978-90-481-3426-7_10.

Rodríguez, L., Vives, L., & Gomez, A. (2013). Conceptual and numerical modeling approach of the Guarani Aquifer System. *Hydrology and Earth System Sciences, 17*, 295-314. http://dx.doi.org/10.5194/hess-17-295-2013.

Saar, M. O. (2011). Review: geothermal heat as a tracer of large-scale groundwater flow and as a means to determine permeabiltiy fields. *Hydrogeology Journal, 19*(1), 31-52. http://dx.doi.org/10.1007/s10040-010-0657-2.

Santarosa, L. L., Gastmans, D., Sitolini, T. P., Kirchheim, R. E., Betancur, S. B., Oliveira, M. E. D., Campos, J. C. V., & Manzione, R. L. (2021). Assessment of groundwater recharge along the Guarani aquifer system outcrop zone in São Paulo State (Brazil): an

important tool towards integrated management. *Environmental Earth Sciences*, *80*, 95. http://dx.doi.org/10.1007/s12665-021-09382-3.

Scanlon, B. R., Keese, K. E., Flint, A. L., Flint, L. E., Gaye, C. B., Edmunds, W. M., & Simmers, I. (2006). Global synthesis of groundwater recharge in semiarid and arid regions. *Hydrological Processes*, *20*(15), 3335-3370. http://dx.doi.org/10.1002/hyp.6335.

Schenato, L. (2017). A review of distributed fiber optic sensors for geo-hydrological applications. *Applied Sciences*, *7*(9), 896. http://dx.doi.org/10.3390/app7090896.

Schmidt, C., Bayer-Raich, M., & Schirmer, M. (2006). Characterization of spatial heterogeneity of groundwater-stream water interactions using multiple depth streambed temperature measurements at the reach scale. *Hydrology and Earth System Sciences*, *10*(6), 849-859. http://dx.doi.org/10.5194/hess-10-849-2006.

Schmidt, C., Conant, B., Bayer-Raich, M., & Schirmer, M. (2007). Evaluation and field-scale application of an analytical method to quantify groundwater discharge using mapped streambed temperatures. *Journal of Hydrology*, *347*(3-4), 292-307. http://dx.doi.org/10.1016/j.jhydrol.2007.08.022.

Selker, J. S., Thévenaz, L., Huwald, H., Mallet, A., Luxemburg, W., van de Giesen, N., Stejskal, M., Zeman, J., Westhoff, M., & Parlange, M. B. (2006b). Distributed fiber-optic temperature sensing for hydrologic systems. *Water Resources Research*, *42*(12), W12202. http://dx.doi.org/10.1029/2006WR005326.

Selker, J., van de Giesen, N., Westhoff, M., Luxemburg, W., & Parlange, M. B. (2006a). Fiber optics opens window on stream dynamics. *Geophysical Research Letters*, *33*(24), L24401. http://dx.doi.org/10.1029/2006GL027979.

Sensornet. (2022). Retrieved in 2022, September 12, from https://www.sensornet.co.uk/wp-content/uploads/2016/05/oryx-data-sheet.pdf

Sharda, V. N., Kurothe, R. S., Sena, D. R., Pande, V. C., & Tiwari, S. P. (2006). Estimation of groundwater recharge from water storage structures in a semi-arid climate of India. *Journal of Hydrology*, *329*, 224-243. http://dx.doi.org/10.1016/j.jhydrol.2006.02.015.

Sindico, F., Hirata, R., & Manganelli, A. (2018). The Guarani Aquifer System: from a beacon of hope to a question mark in the governance of transboundary aquifers. *Journal of Hydrology: Regional Studies*, *20*, 49-59. http://dx.doi.org/10.1016/j.ejrh.2018.04.008.

Sophocleous, M. (2002). Interactions between groundwater and surface water: the state of the science. *Hydrogeology Journal*, *10*(1), 52-67. http://dx.doi.org/10.1007/s10040-001-0170-8.

Stallman, R. W. (1960). Notes on the use of temperature data for computing groundwater velocity. *U.S. Geological Survey*, *39*. Groundwater notes 39.

Sugg, Z. P., Varady, R. G., Gerlak, A. K., & Grenade, R. (2015). Transboundary groundwater governance in the Guarani Aquifer System: reflections from a survey of global and regional experts. *Water International*, *40*(3), 377-400. http://dx.doi.org/10.1080/02508060.2015.1052939.

Swanson, T. E., & Cardenas, M. B. (2011). Ex-Stream: a MATLAB program for calculating fluid flux through sediment–water interfaces based on steady and transient temperature profiles. *Computers & Geosciences*, *37*(10), 1664-1669. http://dx.doi.org/10.1016/j.cageo.2010.12.001.

Thomas, B. F., Caineta, J., & Nanteza, J. (2017). Global assessment of groundwater sustainability based on storage anomalies. *Geophysical Research Letters*, *44*, 11445-11455. http://dx.doi.org/10.1002/2017GL076005.

Tinker, C. J., & Kirchheim, R. E. (2016). The Guarani Aquifer Agreement (Acordo Aquífero Guarani): protection and management of transboundary underground water resources in a regional context. In C. Derani & M. C. Scholz (Eds.), *Mudanças climáticas e recursos genéticos: regulamentação jurídica na COP21* (pp. 39-57). FUNJAB: Florianópolis.

Tyler, S. W., Selker, J. S., Hausner, M. B., Hatch, C. E., Torgersen, T., Thodal, C. E., & Schladow, S. G. (2009). Environmental temperature sensing using Raman spectra DTS fiber-optic methods. *Water Resources Research*, *45*(4), W00D23. http://dx.doi.org/10.1029/2008WR007052.

Vandenbohede, A., Louw, P. G. B., & Doornenbal, P. J. (2014). Characterizing preferential groundwater discharge through boils using temperature. *Journal of Hydrology*, *510*, 372-384. http://dx.doi.org/10.1016/j.jhydrol.2014.01.006.

Wendland, E., Barreto, C., & Gomes, L. H. (2007). Water balance in the Guarani Aquifer outcrop zone based on hydrogeologic monitoring. *Journal of Hydrology*, *342*(3-4), 261-269. http://dx.doi.org/10.1016/j.jhydrol.2007.05.033.

Wendland, E., Gomes, L., & Troger, U. (2015). Recharge contribution to the Guarani Aquifer System estimated from the water balance method in a representative watershed. *Anais da Academia Brasileira de Ciências*, *87*, 52-68. http://dx.doi.org/10.1590/0001-3765201520140062.

Yao, Y., Huang, X., Liu, J., Zheng, C., He, X., & Liu, C. (2015). Spatiotemporal variation of river temperature as a predictor of groundwater/surface-water interactions in an arid watershed in China. *Hydrogeology Journal*, *23*, 999-1007. http://dx.doi.org/10.1007/s10040-015-1265-y.

Authors contributions

Edson Cezar Wendland: Was responsible for the conceptualization, investigation, supervision project administration, and funding acquisition.

Alan Reis: Worked on the methodology, formal analysis, data curation, visualization, writing - original draft paper and writing – review and editing.

Jamil Alexandre Ayach Anache: Worked on the methodology, formal analysis, data curation, visualization, writing - original draft paper and writing – review and editing.

David Maycon Schimdt Rosa: Worked on the investigation and data curation.

Gabriel de Miranda Alcântara: Worked on the investigation and data curation.

Christopher Scott Lowry: Was responsible for the conceptualization, investigation, resources, and writing – review and editing.

Yu-Feng Forrest Lin: Was responsible for the conceptualization, investigation, resources, and writing – review and editing.